frontiers | Frontiers in Energy Research

TYPE Original Research
PUBLISHED 30 May 2023
DOI 10.3389/fenrg.2023.1169468

OPEN ACCESS

EDITED BY
Mohamad Ghaffarian Niasar,
Delft University of Technology,
Netherlands

REVIEWED BY
Babak Gholizad,
Tennet, Netherlands
Armando Rodrigo,
Universitat Politècnica de València, Spain

*CORRESPONDENCE
Weifeng Sun,
weifeng.sun@ntu.edu.sg

RECEIVED 19 February 2023
ACCEPTED 09 May 2023
PUBLISHED 30 May 2023

CITATION
Li Z, Zhang J, Chen S, Liu H, Wang L, Liang J, Zhang K, Zhang P and Sun W (2023), Nonlinear electric conduction of CCTO/EPDM composites used for reinforced insulation in cable accessory. *Front. Energy Res.* 11:1169468. doi: 10.3389/fenrg.2023.1169468

Nonlinear electric conduction of CCTO/EPDM composites used for reinforced insulation in cable accessory

Zhongyuan Li[1], Jian Zhang[1], Shiyu Chen[1], Heqian Liu[1], Lei Wang[1], Jianquan Liang[1], Kexin Zhang[1], Peng Zhang[1] and Weifeng Sun[2]*

[1]Electric Power Research Institute, State Grid Heilongjiang Electric Power Co., Ltd., Harbin, China, [2]School of Electrical and Electronic Engineering, Nanyang Technological University, Singapore, Singapore

Nonlinear electric conductance of reinforced insulation can homogenize electric field distribution and suppress local electric field distortion inside high-voltage direct current cable accessories. To achieve a significant nonlinear electric conductance in ethylene–propylene–diene misch–polymere (EPDM) used for reinforced insulation of cable accessories, the inorganic micron crystal powder of calcium copper titanate (CCTO) is synthesized by the sol–gel method, which is filled into EPDM to prepare 5~15 wt% CCTO/EPDM composites by melting blend and hot-press molding methods. Microscopic structure, electric conductivity, direct current (DC) dielectric breakdown strength, and charge trap characteristics of CCTO/EPDM composites are tested to reveal the underlying derivation of electric conduction nonlinearity. Scanning electron microscopy and X-ray diffraction (XRD) demonstrate that CCTO micron fillers are uniformly dispersed in the EPDM matrix. Dielectric breakdown strength of CCTO/EPDM composites gradually decreases with the increase in CCTO content while persisting qualified for electrical insulation of DC cable accessories. CCTO crystal macron fillers introduce shallower charge traps than the intrinsic charge traps derived from the structural defect EPDM matrix, which initiates the percolating conductive channels between charge traps under high electric fields, accounting for the significant nonlinearity in the profile of electric current density *versus* electric field strength. Finite-element simulations and analyses on the electrostatic field in DC cable terminals prove that employing 15 wt% CCTO/EPDM composite as reinforced insulation can efficiently homogenize the electric field at the interface between the main insulation and accessory insulation of power cables, which is of great interest to develop insulation materials used for DC cable accessories in severe environments.

KEYWORDS

power cable accessory, EPDM, charge trap, reinforced insulation, electric conduction nonlinearity, CCTO

1 Introduction

With the rapid development of new energy sources, such as offshore wind power and photovoltaic power generation, the high-voltage direct current (HVDC) cable has attracted great attention to meet the power transmission demand of long distance, large capacity, and low loss (Ibrahim, 2012; Harry, 2013; Morshuis et al., 2015; Mazzanti, 2017; Chen et al.,

2021). Cable accessory in HVDC transmission systems is essential connection equipment with a complex structure that is composed of multiple insulating layers. Therefore, the coupling relationship between the electrical, mechanical, and thermal performances of different insulating media should be focused on in the design and manufacturing of cable accessories (Li and Du, 2018). As indicated by authentic reports, more than 60% of operation faults in 110 and 220 kV alternative current (AC) cable lines are derived from insulation failures of cable accessories, implying cable accessory is the weakest part in power cables (Zhang et al., 2020).

Ethylene–propylene–diene misch–polymere (EPDM) is the copolymer composed of ethylene, propylene, and a small amount of non-conjugated dienes, for which the commonly used third monomer is methylene norbornene (ENB), dicyclopentadiene (DCPD), or 1,4-hexadiene (HD), whereas the polymeric backbone is constructed by the saturated bonds of chemical stabilizers with side molecular-chains containing unsaturated double bonds. EPDM merits with low loss and high resistance to partial discharge and ultraviolet radiation have been widely utilized in high-voltage cable accessories (Li and Li, 2019; Ohki et al., 2022). Cable accessories contain a complex of interface structures, especially between the main insulation and reinforced insulation, where the electrical performance of the insulation medium abruptly varies in order to be vulnerable to accumulating space charges. Local electric field distortion can preferentially occur at the interface between individual components of cable accessories under DC voltage, which can be homogenized by optimizing geometry configurations or improving the dielectric performances of individual insulation layers. Optimizing the insulation configuration of cable accessories relies highly on the early design of power equipment to increase design cost, whereas improving the dielectric performances of insulation materials is more suitable for ameliorating electrical matching between all the components in cable accessories.

By blending micron fillers of inorganic materials, such as silicon carbide, zinc oxide, and carbon black, composite materials with nonlinear current–voltage characteristics (electric conduction nonlinearity) can be prepared to successfully homogenize the electric field internal cable accessories (Weida et al., 2009; Christen et al., 2010; Xiao et al., 2020). Electric conduction in the SiC/EPDM composite under high direct current electric field shows obvious field-dependent nonlinearity because SiC micron fillers introduce amounts of shallow charge traps, which can also effectively inhibit space charge accumulations at the interface between the reinforced insulation of EPDM and the main insulation of cross-linked polyethylene (XLPE) in cable accessories (Li et al., 2017). ZnO nanofillers synthesized in SnF_2 or $SnCl_2$ aqueous solutions have been used for preparing ZnO/EPDM nanocomposites with an evident electric conduction nonlinearity (Can-Ortiz et al., 2021). In order to obtain significant nonlinear electric conductance and simultaneously improve the mechanical strength of polymeric insulation materials, it is necessary to blend a considerable amount of inorganic fillers with high electric conduction nonlinearity into a polymer matrix, which can reduce the threshold electric field strength of nonlinear electric conductance but cause an inevitable decrease in dielectric breakdown strength. Moreover, the crystallographic structure and preparation process of inorganic fillers greatly account for the dielectric performances of polymer matrix composites. Therefore, it is of great interest to acquire stable insulation performances of polymer dielectric composites by targeting the special species of nonlinear fillers. In addition, Suzana et al. (2014) investigated the effect of carbon black content on EPDM/NBR blends. The results show that the increase in the carbon black content improves the mechanical and radiation properties of EPDM/NBR blend rubber (Suzana et al., 2014).

Copper titanate ($CaCu_3Ti_4O_{12}$, CCTO) with a giant dielectric constant of ~10^4 and a considerable electric conduction nonlinearity has been successfully applied to ultra dielectric capacitors (Chung et al., 2004; Singh et al., 2014). Adopting an appropriate sintering time or cooling rate can effectively improve the electrical properties of CCTO ceramics. For instance, delaying sintering heat preservation or quenching cooldown can significantly increase the dielectric permittivity of CCTO ceramics (Huang et al., 2013). CCTO nanorods represent an explicit electric conduction nonlinearity under external electric fields, which are suitable for electric resistance switches (Tararam et al., 2011). In the present study, a CCTO micron crystal powder with significant electric conduction nonlinearity is successfully synthesized using the sol–gel method to be filled into EPDM for preparing CCTO/EPDM composites, which represent an evident nonlinear electric conductance and persist an adequately high dielectric breakdown strength for reinforced insulation in cable accessories. The charge transport mechanism is elucidated by the charge trapping mechanism and the percolation conductance theory. Thermal–electrical coupling finite-element simulations are implemented to validate CCTO/EPDM composites as a reinforced insulation material for homogenizing electric field internal cable joints or cable terminals.

2 Experiment and simulation methodology

2.1 Material preparation

Copper nitrate and calcium nitrate in a 3:1 mol ratio as a coordinate solute of a total of 28.82 g and tetrabutyl titanate of 41 ml are mixed with an ethylene glycol methyl ether solvent of 160 ml under heating and stirred enough to acquire a uniform solution, which is then preserved for 12 h at room temperature and dark environment. The prepared sol solution is placed in an 80°C thermostatic oven until the solvent completes evaporation to obtain CCTO gel powder, which is then heated up to 950°C and kept for 8 h in a muffle furnace to obtain CCTO crystal powder. Finally, the CCTO micron crystal particles are achieved after the CCTO crystal powder is ground for 12 h under a rotation rate of 500 r/min in a ball miller and then dried at 80°C for 24 h in an electric blast cabinet to completely volatilize alcohol.

By means of melting blend and hot-press molding methods, the CCTO/EPDM composite material is prepared with EPDM (4725P, American DuPont Co. Ltd., Chicago, United States) as the matrix material and dicumyl peroxide (DCP, Nobel Co., Ltd., Aksu, China) as the vulcanizing agent: 1) both EPDM raw material and CCTO micron crystal powder are hot-dried at 60°C for 24 h in vacuum oven to get rid of moisture; 2) the

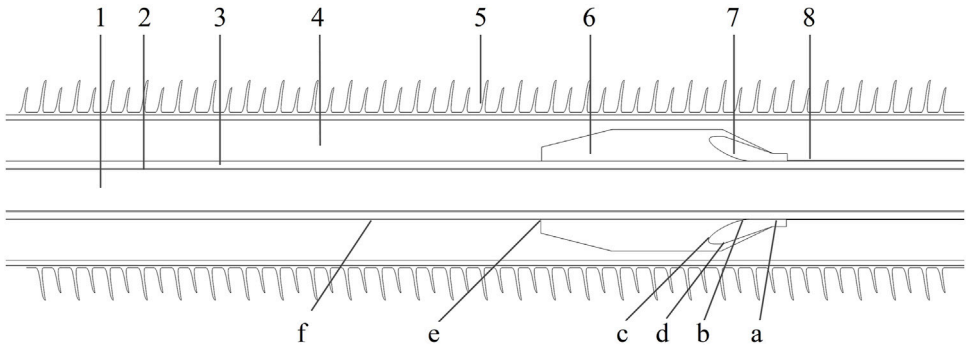

FIGURE 1
Geometry for modeling HVDC cable terminal. 1, conductive core; 2, inner shield; 3, XLPE main insulation; 4, silicone oil; 5, ceramic tube; 6, reinforced insulation; 7, stress cone; 8, outer shield; a, stress cone front terminal; b, stress cone root; c,d, stress cone interface; e, common point of main insulation, silicone oil, and reinforced insulation.

TABLE 1 Dimensions of individual components in the cable terminal.

Component	Dimension (mm)
Core radius	19
XLPE thickness	16
Reinforced insulation thickness	64
Shield layer thickness	1
Axial length of stress cone	160

after-hot-dried EPDM material, 5~15 wt% CCTO micron crystal powder, and 2 phr DCP are mixed into a torque rheometer (RM200C, Hapro Co., Ltd., Harbin, China) to be blended at 100°C for 10 min under a rotation rate of 60 r/min; 3) the obtained raw blend is hot-pressed under 15 MPa for 15 min at 110°C to melting in a plate vulcanizer and then heated by a rate of 5°C/min up to 175°C and kept for 30 min in which the EPDM cross-linking process is fulfilled; and 4) the cross-linked EPDM filled with CCTO micron crystal in a film material of 0.2 ± 0.02 mm thickness is finally cooled down to room temperature and hot-degassed for 3 days at 80°C in a vacuum oven to remove by-product small molecules and release thermal stresses.

2.2 Microstructure characterization and dielectric performance test

A scanning electron microscope (SU8020, Hitachi High-Technologies Corp. Japan) is used to observe the cross-section surface obtained by breaking brittle samples in liquid nitrogen, by which the dispersion of CCTO micro-crystal in the EPDM matrix can be characterized. The crystal structure of the CCTO micron crystal and amorphous short-range order of the EPDM matrix in the CCTO/EPDM composites are characterized using an X-ray diffractometer (Empyrean, PANalytical Corp. Netherlands) compared to the CCTO micron crystal powder. The X-ray diffraction (XRD) test is performed with an electron emission target of Cu (wavelength = 0.15418 Å) under 40 mA electric current and 40 kV voltage in an angular scanning range of 20°~80° by a step of 0.0065° at room temperature.

Dielectric spectra are tested with a wide-frequency dielectric spectrometer (Concept 80, Novocontrol Technologies GmbH & Co., KG, Germany) in a 1~10^6 Hz frequency range at room temperature. Electric conductivity is tested on 100 × 100 mm^2 square film samples of 0.2 mm thickness under 10^6~4 × 10^7 V m^{-1} electric fields at a temperature range of 30~70°C in a three-electrode system (Huang et al., 2013), in which the measured electric conduction current is required to be stable after applying DC voltage for 30 min at each testing point of electric field strength.

Direct current (DC) electric breakdown experiments are implemented at relatively high and low temperatures of 70°C and 30°C on circular film samples of 0.15 mm thickness with high-voltage and ground columnar electrodes of 35 and 50 mm diameters, respectively. It should be noted that all electrodes need to be polished before testing. The entire sample–electrode testing system should be immersed in silicon oil when applying voltage to avert surface creepage discharge. For every material species, the electric breakdown experiment is repeated 10 times to statistically analyze the tested data according to the two-parameter Weibull distribution.

TABLE 2 Material properties specified in thermal-electrical coupling finite-element simulations.

Material	Density/ ($g·cm^{-3}$)	Relative dielectric permittivity	Thermal conduction coefficient/ ($W·m^{-1}·K^{-1}$)	Heat capacity J/(kg·K)
XLPE	910	2.27	1,640	0.285
Inner shield	950	100	2,500	0.510

10.3389/fenrg.2023.1169468

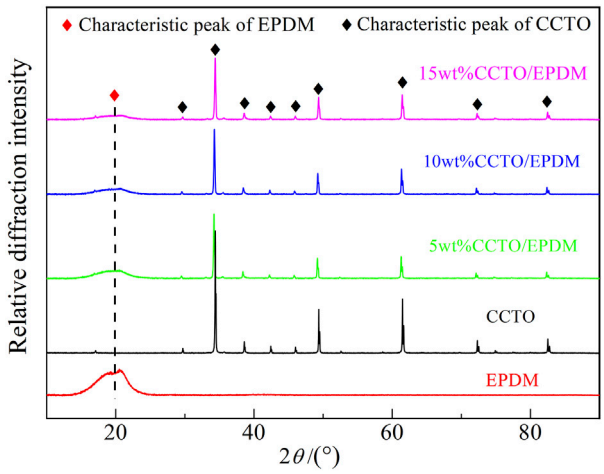

FIGURE 2
XRD angle spectra of CCTO micro-crystal powder and 5~15 wt% CCTO/EPDM composites.

To elucidate charge trap level distribution in the energetic spectrum, the thermal stimulation depolarization current (TSDC) as a function of temperature is tested on film samples of 100 ± 10 μm thickness in a temperature-controlling dual-electrode vacuum system. The tested sample is first polarized under an electric field of 30 kV/mm for 30 min at room temperature and then promptly cooled down to −20°C in a liquid nitrogen environment, after which short-circuit depolarization current is measured when sample chamber temperature is gradually increased to 120°C by a heat rate of 3°C/min.

2.3 Finite-element thermal-coupled electrostatic field simulation

Steady-state calculations of electric fields in a cable accessory under thermo-electric coupling loads are implemented by COMSOL Multiphysics software. The HVDC cable prefabricated terminal at 200-kV voltage level consisting of conduction-nonlinear reinforced insulation, XLPE main insulation, and silicone oil-filled insulation is modeled according to the 2D axis-symmetrical geometry, as shown in Figure 1 and Table 1 (Li et al., 2019). The cable terminal model with an entire length of 2,600 mm is centered by a conductive core for applying DC voltage and outside surrounded by an air environment domain, with the inner edge of the semi-conductive outer shield specified as an electrical ground. For thermal-coupled electrostatic field simulations by the finite-element differential method, the conductive core is specified by a constant temperature of 70°C, and the air environment domain is specified with a convection heat transfer of 10 W/(m^2·K) and a constant temperature of 20°C. Material property specifications on XLPE main insulation and inner shield layer for electrical-thermal coupling simulations are listed in Table 2. The variations of electric conductivity with temperature and field strength are fitted by piecewise cubic spline interpolation functions, and the fitting results are introduced into the cable accessory model for specifying the material properties of reinforced insulation and XLPE main insulation. Delaunay triangulation algorithm of exploiting free triangular elements is adopted for finite-element meshing, with an element size growth rate of 1.5 and a narrow domain relaxation rate of 1.0, which is further refined in the positions where electric field strength and temperature change greatly at multi-layer

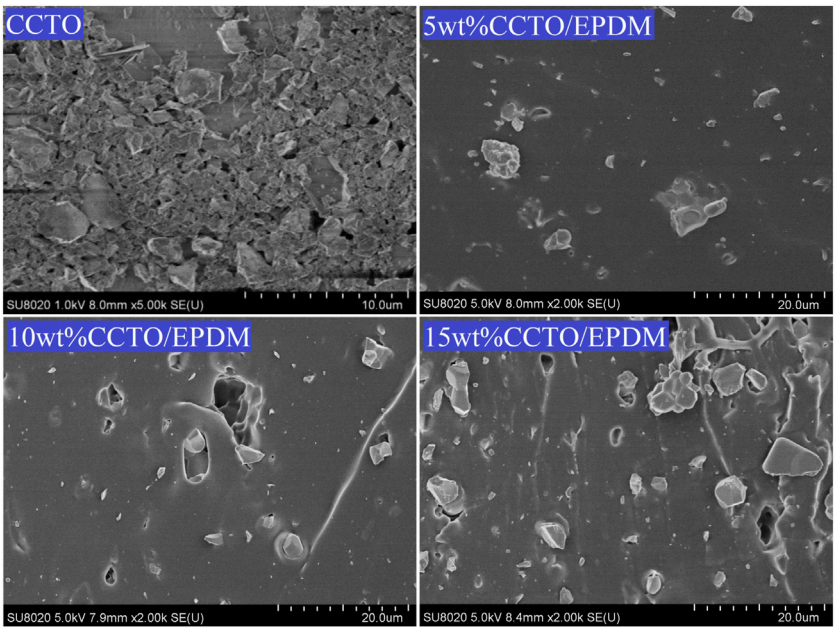

FIGURE 3
Cross-sectional SEM images of CCTO micron crystal powder and 5~15 wt% CCTO/EPDM composites.

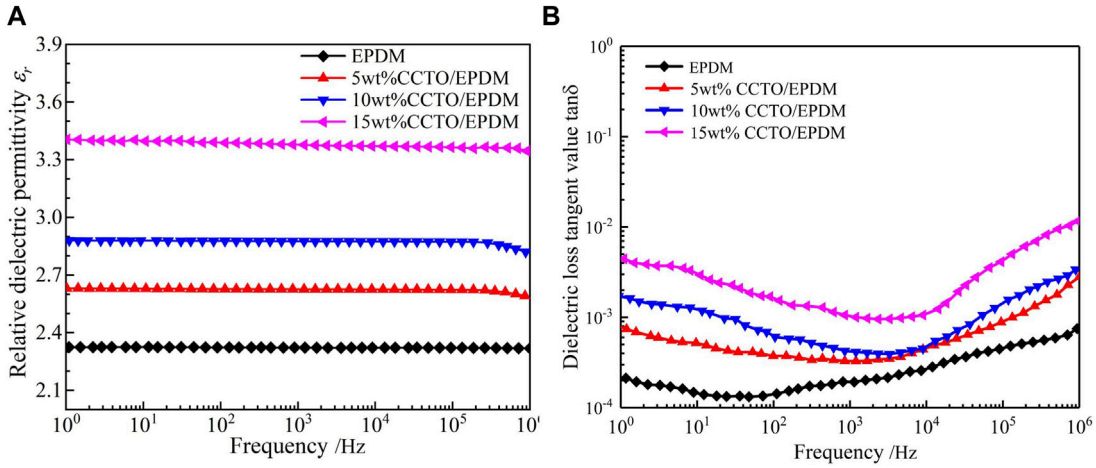

FIGURE 4
Dielectric property of CCTO/EPDM composites as a function of frequency. **(A)** ε_r. **(B)** tanδ.

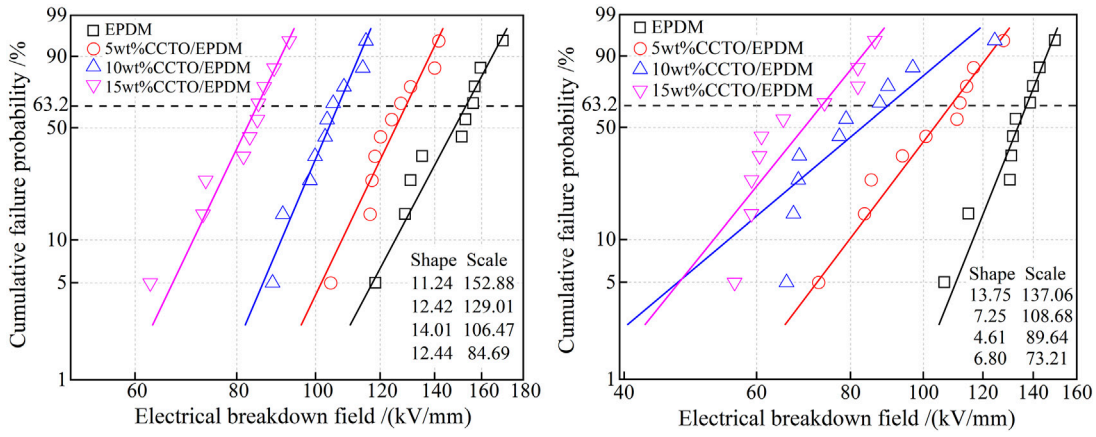

FIGURE 5
DC dielectric breakdown strength of CCTO/EPDM composites at 30°C (left panel) and 70°C (right panel).

interfaces in the cable terminal model. The maximum and minimum numbers of triangular elements are adjusted until all obtuse angles disappear.

3 Results and discussion

3.1 XRD and SEM characterizations

XRD spectra of the CCTO micron crystal powder and 5~15 wt% CCTO/EPDM composites, as shown in Figure 2, indicate that CCTO micron crystals in both pure CCTO powder and CCTO/EPDM composites are in high purity without any impurity crystalline phase that may be generated from air oxygenation on the surface or chemical reaction at composite interfaces. Characteristic diffraction peaks of CCTO crystal fillers in the CCTO/EPDM composite are consistent with those of the pure CCTO powder. For higher CCTO filling content, the CCTO/EPDM composite represents a comprehensively higher intensity of CCTO characteristic peaks and a notably lower intensity of the EPDM characteristic peak. Accordingly, it is demonstrated by XRD characterizations that CCTO micron crystal fillers are mixed physically into EPDM without any chemical reaction at composite interfaces.

As illustrated by the cross-sectional SEM images of CCTO micron crystal powder and CCTO/EPDM composites in Figure 3, CCTO fillers with uniform sizes of 3~5 μm, despite being in irregular shapes, disperse uniformly in 5 wt% and 10 wt % CCTO/EPDM composites without filler agglomeration while showing a minority of agglomeration under 15 wt% filling content.

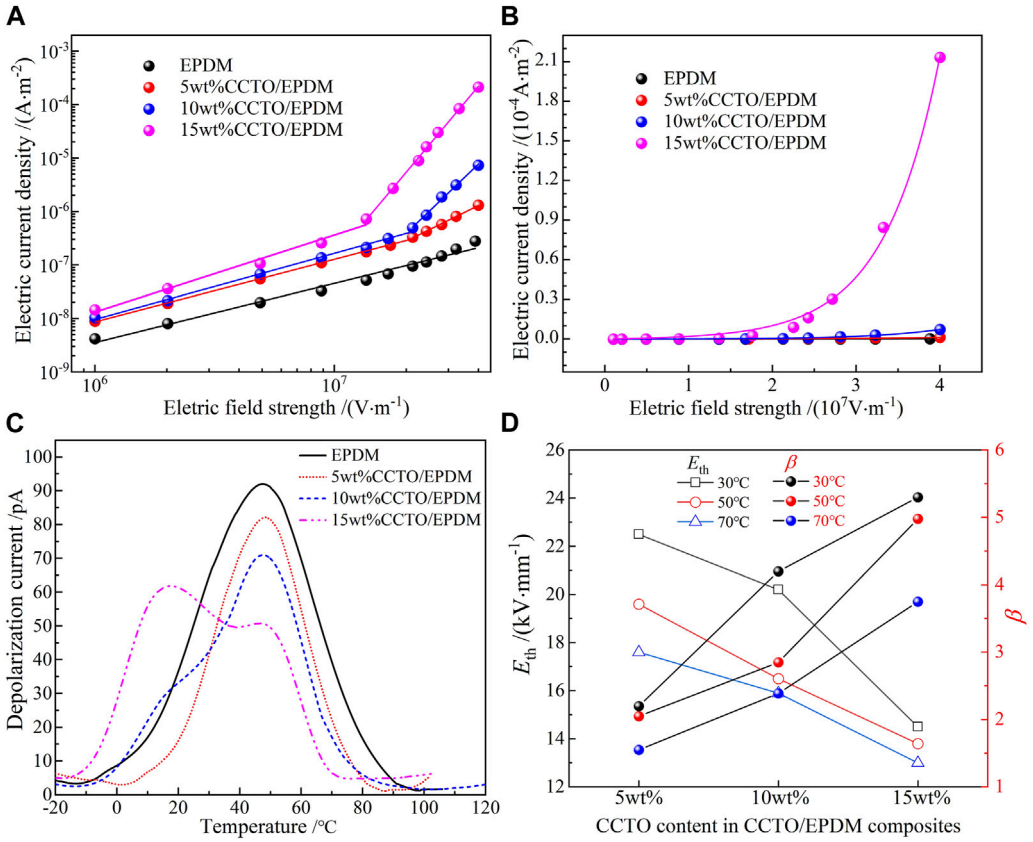

FIGURE 6
(A) Electric conduction *J*-*E* characteristics of CCTO/EPDM composites in double logarithmic coordinates for stepwise linear fitting (top-left panel), **(B)** percolation conductance fitting, **(C)** temperature spectra of thermal stimulation depolarizing currents in CCTO/EPDM composites, and **(D)** threshold electric-field strength *E*th and nonlinear coefficient β of CCTO/EPDM composites at various temperatures of 30°C, 50°C, and 70°C.

TABLE 3 Threshold electric field strength *E*th and nonlinear coefficient β of electric conduction in CCTO/EPDM composites.

Material	*E*th/(kV/mm)	β
EPDM	—	—
5 wt% CCTO/EPDM	22.5	2.2
10 wt% CCTO/EPDM	20.2	4.2
15% wtCCTO/EPDM	14.5	5.3

TABLE 4 Carrier hopping distance of percolation conduction in CCTO/EPDM composites.

Material	Hopping distance (nm)
EPDM	2.98
5 wt% CCTO/EPDM	3.61
10 wt% CCTO/EPDM	6.39
15 wt% CCTO/EPDM	7.92

3.2 Dielectric permittivity and breakdown strength

Relative dielectric permittivity of the CCTO/EPDM composite increases evidently with the increase in CCTO filling content, as shown in Figure 4A, which is primarily attributed to the host giant dielectric permittivity of CCTO fillers. Furthermore, the large amount of CCTO/EPDM interfaces introduced by the highly dispersive CCTO micron fillers in the EPDM matrix gives rise to a substantial quantity of interfacial dipoles contributing significantly to the macroscopic dielectric response of CCTO/EPDM composites. Accordingly, a little increase in the CCTO volume or mass content can cause a considerable promotion of the interface area in CCTO/EPDM composites, as manifested by the evident improvement in dielectric permittivity. The dielectric loss of CCTO/EPDM composites gradually increases with the increase in the CCTO content and exhibits a trend of first decreasing and then increasing with frequency, as shown in Figure 4B. As the dielectric loss of insulating material is mainly derived from electric conduction loss at low frequencies, the addition of CCTO crystal powder leads to a significant increase in the electrical conductivity of EPDM, resulting in a larger dielectric loss factor. As the frequency increases, the conduction loss decreases, leading to a decrease in the dielectric loss factor; as the frequency further

10.3389/fenrg.2023.1169468

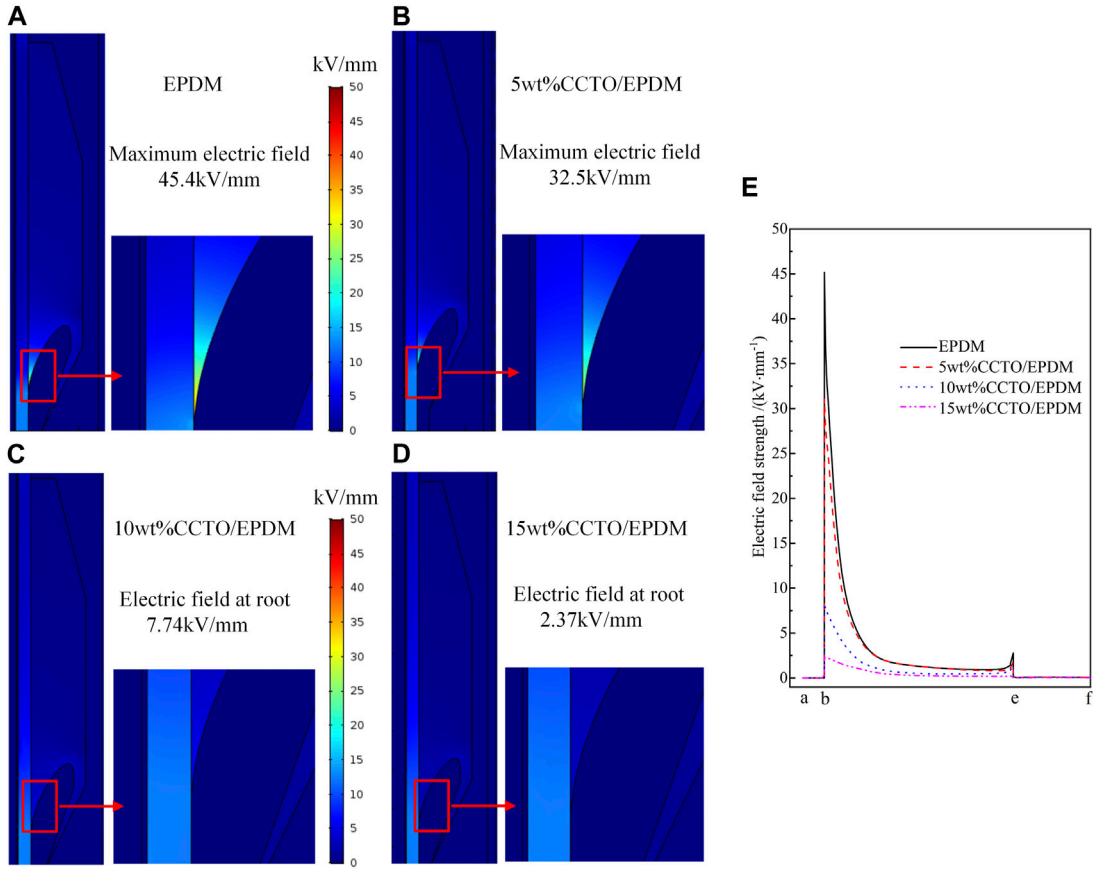

FIGURE 7
Electric field strength **(A–D)** distributed in the cable terminals and **(E)** varying at reinforce-layer/XLPE stress cone interfaces, in which the reinforced insulation layers are hosted by EPDM or 5~15 wt% CCTO/EPDM composites.

increases, the relaxation polarization dominates the dielectric loss, which means the dielectric response cannot keep up with the external alternative electric field, resulting in significant relaxation polarization loss and a further increment in loss factor.

The characteristic breakdown field strength (scale parameter of Weibull distribution) of the CCTO/EPDM composite under DC voltage decreases with the increased CCTO content, approaching 84.70 kV/mm when CCTO content reaches 15 wt%, as shown in Figure 5. Conforming to the electric breakdown theory of solids (Budenstein, 1980), the additional carriers introduced by CCTO macron fillers will exacerbate the electric breakdown process of the EPDM matrix after obtaining adequate kinetic energy to generate impact ionization, which accounts for reducing electric breakdown resistance compared with pure EPDM. Meanwhile, the CCTO content increment leads to the reduction of effective distances between CCTO fillers in the CCTO/EPDM composite, which favors producing percolation conduction channels and results in the degradation of dielectric breakdown strength.

3.3 Nonlinear electric conduction

Electric conduction characteristics profiled by electric current density *versus* electric field strength (*J-E*) of CCTO/EPDM composites represent a critical point at threshold electric field strength *E*th, as shown in Figure 6A. When the applied electric field strength E_{ap} is lower than *E*th, the *J-E* curves in double-logarithmic coordinates are linearly fitted with a slope of 1, which means *J* is linearly dependent of *E*, complying with Ohm's law. For $E_{ap} > E$th, *J* increases exponentially with *E*, as manifested by the linearly fitted slope of $\beta > 1$ (nonlinear coefficient as listed in Table 3) on double-logarithmic *J-E* curves, as a nonlinear electric conductance. Conforming to percolation electric conduction theory (Strümpler and Glatz-Reichenbach, 1999). When CCTO content in the EPDM matrix exceeds the percolation threshold, the distance between CCTO fillers is reduced to form a randomly arising conduction channel, which accounts for the electric conduction nonlinearity of CCTO/EPDM composites. With the increase in CCTO content, the spatial distance and the percolating conduction channel between CCTO fillers become shorter, leading to the abatement in the probability of carrier hopping transports so that a lower threshold electric field strength is needed for initiating percolation electric conductance and a more evident electric conduction nonlinearity will arise. Therefore, higher CCTO content results in lower *E*th and a higher β, and the highest CCTO content of 15 wt% renders the highest electric conduction nonlinearity of CCTO/EPDM composites.

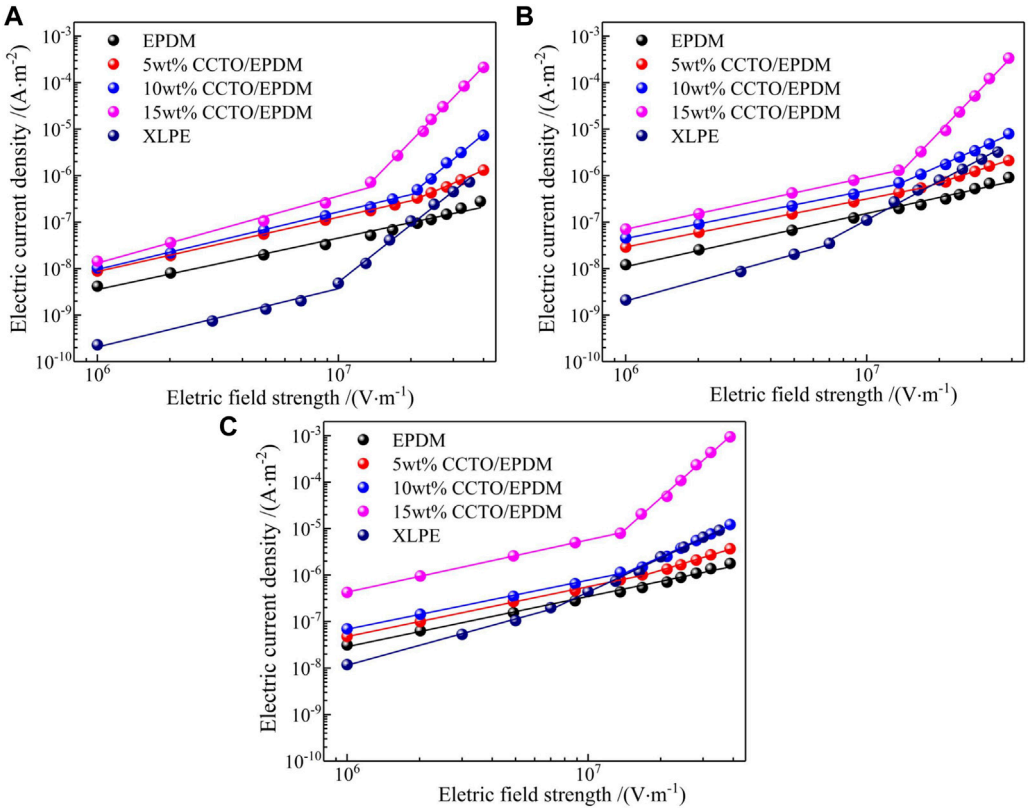

FIGURE 8
Conductivity characteristics of CCTO/EPDM and XLPE at different temperatures: **(A)** 30°C, **(B)** 50°C, and **(C)** 70°C.

Nonlinear composite of inorganic-filler packed polymers has numerous abrupt interfaces, which form multiple bound electron states to be granted as charge traps in various depths from electronic band edges of the polymer matrix. Under thermal excitation or the field-assistant effect, the trapped charge carriers overcome and continuously hop through the energy barriers between charge traps to produce percolating electric conduction (carrier hopping transport), which represents the special relationship between electric current density with electric field and temperature (Taleb et al., 2013):

$$J = 2Ndve\exp\left(-\frac{\delta}{k_bT}\right)\sinh\left(\frac{qlE}{2k_bT}\right), \quad (1)$$

where J denotes electric current density, N signifies the density of carriers directly participating in DC electric conduction, v and l indicate charge hopping probability and distance, respectively, q is the fundamental charge quantity, δ symbolizes activation energy, E denotes the applied electric field strength, and k_b is the Boltzmann constant. *J-E* curves in linear coordinates of EPDM and CCTO/EPDM composites are fitted according to the percolating electric conduction described by Eq. 1, as shown in Figure 6B and Table 4. The temperature spectra of TSDC, characterizing the energetic distribution of charge trap density, indicate that CCTO fillers introduce amounts of shallower charge traps into EPDM, the density of which can be increased by raising CCTO filling content, as shown in Figure 6C. It should be noted that the charge carriers injected from electrodes are preferentially captured by the shallower traps introduced by CCTO fillers and will then begin to be captured into the intrinsic deeper charge traps derived from structural defects of the EPDM matrix. Compared with pure EPDM, the shallower charge traps in CCTO/EPDM composites imply a shorter carrier hopping distance in percolating electric conduction, resulting in a higher electric conductivity and a more significant *J-E* nonlinearity, as indicated in the >5 wt% CCTO/EPDM composites. Most shallow traps in polymer composites exist in interface regions (Tanaka et al., 2004; Tanaka et al., 2005), and the appreciable increment of dielectric permittivity is an actual indication of the significant interfacial polarization introduced by filling CCTO micron crystals into EPDM, demonstrating the great amounts of interface structures existing in CCTO/EPDM composites. As a result, the density of shallow traps in CCTO/EPDM composites increases notably with the increase in CCTO content. As shown by the temperature dependence of electric conduction characteristics in Figure 6D, Eth and β decrease with the elevated temperature, which is the substantial verification of percolation electric conductance accounting for electric conduction nonlinearity of CCTO/EPDM composites. As described by Eq. 1, the trapped charge carriers undergo hopping transports under thermal excitation, which means the temperature dependence of hopping probability in a percolation process follows the Boltzmann distribution (thermal excitation function), as simply indicated by the more evident electric

conduction nonlinearity of CCTO/EPDM composites at a higher temperature.

3.4 Finite-element simulations on electric fields inside the cable terminal

When EPDM and 5 wt% the CCTO/EPDM composite are used as reinforced insulation, the maximum electric field strengths of 45.4 and 32.5 kV/mm appear at the stress cone root of reinforced insulation in the cable terminal, as shown in Figures 7A, B. In contrast, using 10~15 wt% CCTO/EPDM composites as reinforced insulation reduces the maximum electric field strength to 13.3 kV/mm, which locates in XLPE main insulation of the cable terminal, as shown in Figures 7C, D. In composite dielectrics under an electrostatic field, the electric strength is inversely proportional to electric conductivity. As the electric field strength increases, the conductivity of the CCTO/EPDM composite material with significant electrical conductivity nonlinearity is significantly higher than that of XLPE, as shown in Figure 8. Accordingly, the nonlinear electric conductance of the reinforced insulation layer causes the electric flux through the cable terminal to be concentrated in XLPE main insulation, which is more evident for higher CCTO content. As electric conduction nonlinearity of CCTO/EPDM composites increases significantly with increasing CCTO content, the location of maximum electric field shifts from stress cone root to the XLPE main insulation in the cable terminal when using >5 wt% CCTO/EPDM composites as reinforced insulation material. Although using 10 and 15 wt% CCTO/EPDM composite as reinforced insulation results in almost the same maximum electric field, both located in XLPE main insulation, the electric field strength at the stress cone root of reinforced insulation approaches 7.74 and 2.37 kV/mm (lower than inception electric field strength of 3 kV/mm for surface creepage discharges) respectively, as shown in Figure 7E. Therefore, it is highly suggested to avert creepage discharge on the cable terminal surface using 15 wt% CCTO/EPDM composite as reinforced insulation material.

4 Conclusion

Nonlinear electric conductivity EPDM composites filled with CCTO micron crystal are developed with soluble gel, melting blend, and hot-press molding methods to improve the electrical matching between reinforced insulation and main insulation in the cable terminal. The effect of CCTO fillers on the dielectric properties of EPDM and the underlying mechanism of electric conduction nonlinearity in CCTO/EPDM composites are elucidated by TSDC-derived charge trap characteristics and percolation-attributed electric conductance. It is valid to use CCTO/EPDM composites as reinforced insulation to homogenize the internal electric field of the HVDC cable terminal, verified through thermal-coupling electrostatic field simulations with the finite-element differential method. Increasing the CCTO content can significantly promote nonlinear coefficient and decrease the electric field threshold of arising nonlinear electric conduction in CCTO/EPDM composites while causing a slight decrease in DC dielectric breakdown strength. CCTO fillers are competent in introducing shallow charge traps to initiate charge hopping transports under room-temperature thermal excitation and higher-than-threshold electric field, resulting in a significant electric conduction nonlinearity agreeing well with the percolation conductance mechanism. The electric field strength at the root and surface of the stress cone in the cable terminal decreases evidently with the increase in CCTO content. When CCTO content increases to 15 wt%, it is efficient to use the CCTO/EPDM composite as reinforced insulation to ameliorate electric field distribution and avert surface creepage discharge in the HVDC cable terminal.

Data availability statement

The original contributions presented in the study are included in the article/Supplementary Material. Further inquiries can be directed to the corresponding author.

Author contributions

Data curation, formal analysis, and methodology: ZL; concept, investigation, writing—original draft preparation, and writing—review and editing: WS; project administration and resources: JZ, JL, LW, and KZ. All authors listed made a substantial, direct, and intellectual contribution to the work and approved it for publication.

Funding

This work was supported by the technology project of the State Grid Corporation of Research on Insulation Failure Mechanism and Key Technology of Reliability Improvement for Dry-type Air-core Reactor in Cold Area (Grant no. 5108-202218280A-2-338-XG).

Acknowledgments

The authors thank the Electric Power Research Institute, State Grid Heilongjiang Electric Power Co., Ltd. for supporting this project.

Conflict of interest

ZL, JZ, SC, HL, LW, JL, KZ, and PZ was employed by Electric Power Research Institute, StateGrid Heilongjiang Electric Power Co., Ltd. The authors declare that this study received funding from State Grid Corporation. The funder had the following involvement in the study: data collection and analysis.

The remaining author declares that the research was conducted in the absence of any commercial or financial relationships that could be construed as a potential conflict of interest.

Publisher's note

References

Budenstein, P. P. (1980). On the mechanism of dielectric breakdown of solids. *IEEE Trans. Dielectr. Electr. Insulation* 15 (3), 225–240. doi:10.1109/tei.1980.298315

Can-Ortiz, A., Laudebat, L., Valdez-Nava, Z., and Diaham, S. (2021). Nonlinear electrical conduction in polymer composites for field grading in high-voltage applications: A review. *Polymers* 13 (9), 1370. doi:10.3390/polym13091370

Chen, J., Wu, S., Hu, L. B., Ren, C. Y., and Shao, T. (2021). Analysis of insulation state and physicochemical property of retired high-voltage cable accessories. *Trans. China Electrotech. Soc.* 36 (12), 2650–2658.

Christen, T., Donzel, L., and Greuter, F. (2010). Nonlinear resistive electric field grading part 1: Theory and simulation. *IEEE Electr. Insul. Mag.* 26 (6), 47–59. doi:10.1109/mei.2010.5599979

Chung, S. Y., Kim, I. D., and Kang, S. J. L.(2004). Strong nonlinear current-voltage behaviour in perovskite-derivative calcium copper titanate. *Nat. Mater.* 3 (11), 774–778. doi:10.1038/nmat1238

Harry, O. (2013). History of underground power cables. *IEEE Electr. Insul. Mag.* 29 (4), 52–57. doi:10.1109/mei.2013.6545260

Huang, Y. M., Shi, D. P., Li, Y. H., Li, G. Z., Wang, Q. C., Liu, L. J., et al.(2013). Effect of holding time on the dielectric properties and non-ohmic behavior of $CaCu_3Ti_4O_{12}$ capacitor-varistors. *J. Mater. Sci. Mater. Electron.* 24 (6), 1994–1999. doi:10.1007/s10854-012-1047-4

Ibrahim, A. M. (2012). The evolution of medium voltage power cables. *IEEE Potentials* 31 (3), 20–25. doi:10.1109/mpot.2011.2178190

Li, C. C., and Li, P. J. (2019). Application of calcined clay in EPDM wire and cable compound. *Rubber Sci. Technol.* 17 (3), 168–172.

Li, J., Du, B., Kong, X. X., and Li, Z. L.(2017). Nonlinear conductivity and interface charge behaviors between LDPE and EPDM/SiC composite for HVDC cable accessory. *IEEE Trans. Dielectr. Electr. Insulation* 24 (3), 1566–1573. doi:10.1109/tdei.2017.006198

Li, Z. L., and Du, B. X. (2018). Polymeric insulation for high-voltage dc extruded cables: Challenges and development directions. *IEEE Electr. Insul. Mag.* 34 (6), 30–43. doi:10.1109/mei.2018.8507715

Li, Z. Y., Sun, W. F., and Zhao, H. (2019). Significantly improved electrical properties of photo-initiated auxiliary crosslinking EPDM used for cable termination. *Polymers* 11 (12), 2083. doi:10.3390/polym11122083

Mazzanti, G. (2017). Life and reliability models for high voltage DC extruded cables. *IEEE Electr. Insul. Mag.* 33 (4), 42–52. doi:10.1109/mei.2017.7956632

Morshuis, P., Cavallini, A., Fabiani, D., Montanari, G., and Azcarraga, C. (2015). Stress conditions in HVDC equipment and routes to in service failure. *IEEE Trans. Dielectr. Electr. Insulation* 22 (1), 81–91. doi:10.1109/tdei.2014.004815

Ohki, Y., Hirai, N., and Okada, S. (2022). Penetration routes of oxygen and moisture into the insulation of FR-EPDM cables for nuclear power plants. *Polymers* 14 (23), 5318. doi:10.3390/polym14235318

Singh, A. P., Saxena, S., and Govindan, A. (2014). Studies on the dielectric constant and conductivity of $CaCu_3Ti_4O_{12}$: PET and $CaCu_3Ti_4O_{12}$: PVC ceramic polymer composites. *Eng. Res. Technol.* 3 (12), 871–874.

Strümpler, R., and Glatz-Reichenbach, J. (1999). Conducting polymer composites. *J. Electroceramics* 3 (4), 329–346. doi:10.1023/a:1009909812823

Suzana, S.-J., Vojislav, J., Milena, M.-C., Jaroslava, B.-S. G. M., and Marković, G. (2014). Comparative study of radiation effect on rubber-carbon black compounds. *J. Compos. Part B* 62, 183–190. doi:10.1016/j.compositesb.2014.02.029

Taleb, M., Teyssedre, G., Roy, S. L., and Laurent, C. (2013). Modeling of charge injection and extraction in a metal/polymer interface through an exponential distribution of surface states. *IEEE Trans. Dielectr. Electr. Insulation* 20 (1), 311–320. doi:10.1109/tdei.2013.6451372

Tanaka, T., Kozako, M., Fuse, N., and Ohki, Y. (2005). Proposal of a multi-core model for polymer nanocomposite dielectrics. *IEEE Trans. Dielectr. Electr. Insulation* 12 (4), 669–681. doi:10.1109/tdei.2005.1511092

Tanaka, T., Montanari, G. C., and Mulhaupt, R. (2004). Polymer nanocomposites as dielectrics and electrical insulation-perspectives for processing Technologies, material characterization and future applications. *IEEE Trans. Dielectr. Electr. Insulation* 11 (5), 763–784. doi:10.1109/tdei.2004.1349782

Tararam, R., Joanni, E., Savu, R., Bueno, P. R., Longo, E., and Varela, J. A. (2011). Resistive-switching behavior in polycrystalline $CaCu_3Ti_4O_{12}$ nanorods. *ACS Appl. Mater. Interfaces* 3 (2), 500–504. doi:10.1021/am101079g

Weida, D., Steinmetz, T., and Clemens, M. (2009). Electro-quasistatic high voltage field simulations of large scale insulator structures including 2D models for nonlinear field-grading material layers. *IEEE Trans. Magnetics* 45 (3), 980–983. doi:10.1109/tmag.2009.2012492

Xiao, M., Meng, J., Li, J., Li, Z. L., and Du, B. X. (2020). Electrical properties of $CaCu_3Ti_4O_{12}$-EPDM for cable accessories. *IEEE Trans. Dielectr. Electr. Insulation* 27 (3), 932–938. doi:10.1109/tdei.2020.008525

Zhang, Z. P., Zheng, C. J., Zheng, M., Zhao, H., Zhao, J. K., Sun, W. F., et al.(2020). Interface damages of electrical insulation in factory joints of high voltage submarine cables. *Energies* 13 (15), 3892. doi:10.3390/en13153892